Check for updates

Zitierweise: *Angew. Chem. Int. Ed.* **2024**, *63*, e202319382
doi.org/10.1002/anie.202319382

DNA Nanotechnology | Hot Paper

Synthetic Genes For Dynamic Regulation Of DNA-Based Receptors

Daniela Sorrentino, Simona Ranallo, Eiji Nakamura, Elisa Franco, and Francesco Ricci**

Abstract: We present a strategy to control dynamically the loading and release of molecular ligands from synthetic nucleic acid receptors using in vitro transcription. We demonstrate this by engineering three model synthetic DNA-based receptors: a triplex-forming DNA complex, an ATP-binding aptamer, and a hairpin strand, whose ability to bind their specific ligands can be cotranscriptionally regulated (activated or inhibited) through specific RNA molecules produced by rationally designed synthetic genes. The kinetics of our DNA sensors and their genetically generated inputs can be captured using differential equation models, corroborating the predictability of the approach used. This approach shows that highly programmable nucleic acid receptors can be controlled with molecular instructions provided by dynamic transcriptional systems, illustrating their promise in the context of coupling DNA nanotechnology with biological signaling.

Introduction

Cell-free systems employ cell extracts or purified components (such as enzymes, nucleotides, amino acids and cellular cofactors) to achieve in a highly controlled fashion the in vitro transcription-translation reactions typical of gene expression in living cells. Such systems have recently emerged as simplified yet versatile methods for building biological networks,[1–4] making them an alternative route to cell-based approaches for a variety of applications such as biosensing,[5,6] diagnostics[7–12] and therapeutics. For example, Collins and co-workers have reported several assays for the detection of viral RNAs and small molecules based on the rational design of responsive synthetic genes that, upon target recognition, induce the cell-free translation of a reporter enzyme.[13–15] A ligand-responsive cell-free transcription device (termed ROSALIND) has been also developed for the detection of water contaminants[16] and more recently we have reported the use of transcriptional switches for the detection of specific antibodies.[17–19] Alternatively, cell-free transcription/translation systems have been also used to develop synthetic genetically engineered circuits for different applications,[20–22] including the production of proteins and the development of nucleic acid constructs for gene therapy. In this context, Kim and Winfree have demonstrated genetic regulatory networks in which in vitro transcriptional circuits regulated only by T7 RNA polymerase and RNase H can be used to generate and degrade RNA signals.[23] In other reports, different groups have reported the use of synthetic genes programmed to transcribe RNA aptamers that act as inhibitors or activators of polymerase enzymes.[24,25,26]

In the field of supramolecular chemistry and material science an important goal is to design new synthetic devices that, taking inspiration from biological receptors, can bind a specific molecular ligand and release it in response to a range of different stimuli in a highly controllable fashion.[27,28] Many of these systems, often referred as smart materials or receptors, have been described to date based on the use of imprinted polymers,[29] macrocyclic architectures,[30] and biomimetic host–guest molecules[31] and can find application in molecular transport and drug-delivery.[32] The high predictability of non-covalent interactions, together with the low-cost of synthesis, and biocompatibility make synthetic nucleic acids (DNA or RNA) a suitable engineering material to build similar smart systems and many examples of devices and structures that are able to load a cargo and release it in response to a specific input have been demonstrated so far.[33–35] For example, Dietz and co-workers have recently described an antigen-decorated DNA origami that can reconfigure upon antibody binding[36] thus inducing the release of a viral cargo. In another example, a DNA origami nanocapsule has been designed to open and close in response to pH changes and thus release the enclosed molecular cargo.[37] Simpler DNA-based receptors have been also demonstrated that, through conformational change mechanism, can load or release a molecular cargo in response to small molecules[27,38,39] and nucleic acid strands.[28,41–43]

Engineering such smart DNA systems so that they are able not only to bind a molecular cargo but also to respond to a specific molecular input can be challenging as the responsive domain can conflict with the functional requirements imposed by the ligand-binding receptor. This could ultimately limit the generality of these systems and highlights the need for a strategy that uncouples (also in a spatial fashion) the ligand-binding and responsive functions of DNA-based receptors.

Motivated by the above arguments, here we present a strategy for controlling the loading and release of ligands

[*] D. Sorrentino, S. Ranallo, F. Ricci
Department of Chemistry, University of Rome, Tor Vergata, Via della Ricerca Scientifica, 00133 Rome, Italy
E-mail: francesco.ricci@uniroma2.it
D. Sorrentino, E. Nakamura, E. Franco
Department of Mechanical and Aerospace Engineering and of Bioengineering, University of California at Los Angeles, 420 Westwood Plaza, Los Angeles, California 90095, United States
E-mail: efranco@seas.ucla.edu

© 2024 Wiley-VCH GmbH

from synthetic DNA receptors using cell-free in vitro transcription. We propose here the use of synthetic genes encoding for RNA effector strands (i.e., activators or inhibitors) that, by binding to a synthetic DNA ligand-binding receptor (Figure 1), cause the release or the loading of a ligand by inducing a conformational change that is physically distinct from the sensing domain. With this strategy the receptor is controlled "cotranscriptionally" by the synthetic gene, and efficiently decouples the loading/releasing function of the receptor from the effector function of the gene.

Results and Discussion

As a first model system we used as our synthetic DNA receptor a triplex-forming DNA strand that is designed to bind a 9-nt DNA ligand (light blue, Figure 2) through both Watson–Crick-Franklin and Hoogsteen interactions.[43] To create a genetic mechanism to control our receptor, we first built an effector "release" gene that induces the transcription of an RNA effector strand that acts as an inhibitor for the ligand-binding DNA receptor (blue, Figure 2a). The RNA effector strand is in fact designed to bind to the receptor's loop portion, inducing a conformational change that triggers the release of the DNA ligand (Figure Supporting Information 1). To monitor the load and release of the ligand from the DNA-based receptor we labeled the two ends of the DNA ligand strand with a fluorophore-quencher pair. The formation of the receptor/ligand triplex complex thus results in a significant increase in fluorescence signal upon loading, followed by a decrease in signal when the ligand strand is released from the receptor.

Because the receptor's state can be regulated through an effector that is produced cotranscriptionally (without any RNA purification or annealing step), by simply changing the concentration of the effector "release" gene in solution we can finely regulate the receptor's capacity to recruit its specific ligand. In our experiments we systematically added a fixed amount of T7 RNA polymerase (T7 RNAP, 4 U/μL),

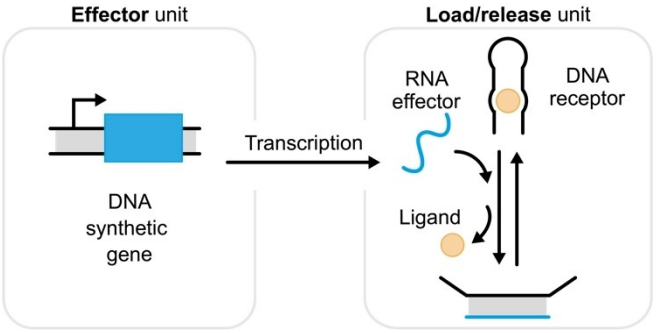

Figure 1. Cotranscriptional control of a synthetic DNA ligand-binding receptor. A DNA synthetic gene (effector unit) is rationally designed to transcribe an RNA strand that acts as effector for a ligand-binding DNA receptor (load/release unit). The binding between the RNA effector and the DNA receptor leads to the controlled release of the ligand from the receptor.

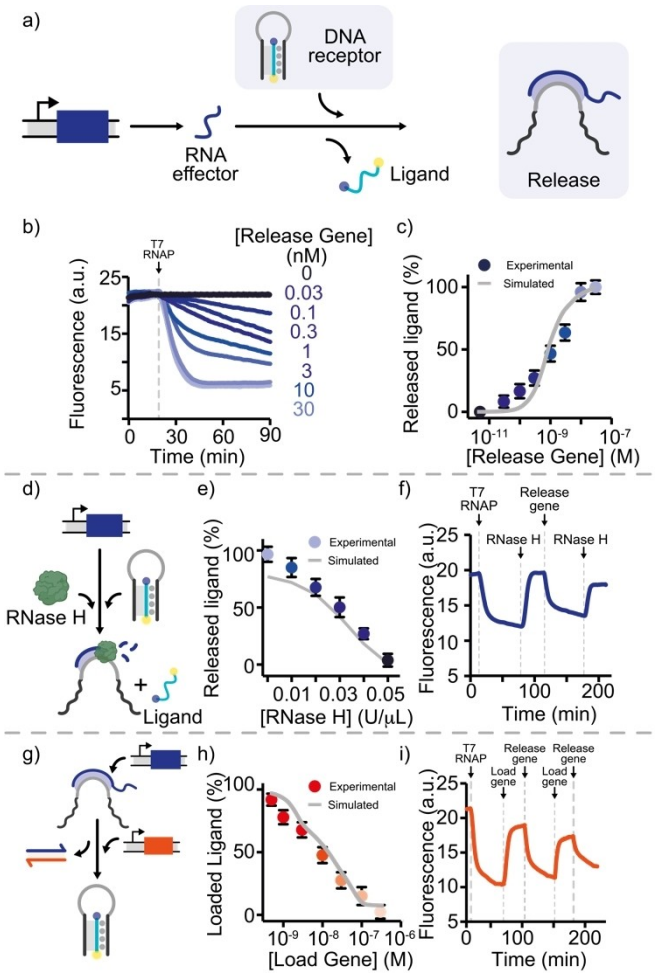

Figure 2. a) General Scheme of our DNA receptor and its RNA effector. b) Time-course experiments testing the effect of varying concentrations of "release" gene. c) Released ligand (%) as a function of effector gene concentration (endpoints of traces like those shown in panel b). d) Schematic of RNase H-controlled release of the DNA ligand from the receptor. e) Released ligand (%) as a function of RNase H concentration ranging from 0.05 U/μL to 0 U/μL (time-course experiments are shown in Figure Supporting Information 3) f) Time-course experiments with successive additions of RNase H (0.05 U/μL) and "release" gene (1 nM). g) Scheme of reversible ligand loading/release. h) Loaded ligand at varying concentrations of the "load" gene in the presence of a fixed concentration of "release" gene (1 nM) (time-course experiments are shown in Figure Supporting Information 5) i) Time-course experiments with sequential additions of "load" (10 nM) and "release" (30 nM) genes. In the graphs, dots represent experimental values while solid gray lines represent fits (c, e, and h) obtained with the kinetic model (see Supporting Information Section Supporting Information 3.2, 3.3). All the experiments in this and the following Figures were performed in 100 mM Tris-HCl, 10 mM $MgCl_2$, 150 mM NaCl at pH 7.0, 37 °C. All transcription reactions were carried out, unless otherwise noted, using DNA-receptor (100 nM), DNA ligand (30 nM), T7 RNAP (4 U/μL). Solid gray lines represent fits (c, e, and h) obtained with the kinetic model (see Supporting Information Section Supporting Information 3.4, 3.5). For clarity, error bars have been shown for only one curve in these and the following figures. The error bars represent the standard deviation of measurements made on at least three independent replicates. Similar relative standard deviations (between 5% and 7%) have been obtained with the other experiments.

© 2024 Wiley-VCH GmbH

15213757, 2024, 17, Downloaded from https://onlinelibrary.wiley.com/doi/10.1002/ange.202319382 by University Of California, Los, Wiley Online Library on [29/09/2024]. See the Terms and Conditions (https://onlinelibrary.wiley.com/terms-and-conditions) on Wiley Online Library for rules of use; OA articles are governed by the applicable Creative Commons License

the enzyme that catalyzes 5′→3′ synthesis of the RNA strand from the gene, to different effector gene concentrations, while maintaining a fixed receptor-ligand ratio. By doing so, we measured a concentration-dependent ligand release that reaches a plateau (98±2 %) at a 30 nM effector gene concentration (Figure 2b,c, Figure Supporting Information 2). We can also control the ligand's release from the receptor by using in the same solution different concentrations of RNase H, an enzyme that specifically degrades RNA strands in DNA-RNA heteroduplexes (Figure 2d). In this case, we observe that ligand release is suppressed at higher RNase H concentrations, and is restored as the concentration of RNase H decreases (Figure 2e, Figures Supporting Information 3, 4). We also demonstrate multiple load/release cycles through the successive addition of the effector gene and of RNase H to a solution containing a fixed concentration of receptor (100 nM), and ligand (30 nM) (Figure 2f). The decrease in the amplitude of fluctuations between cycles, which is more pronounced for RNA transcription, is likely due to the progressive degradation of T7 RNAP and the depletion of necessary substrates (NTPs).

We then introduced a second artificial "load" gene that produces an RNA effector designed to work as an activator for the same DNA triplex-forming receptor. In this case the RNA activator cotranscriptionally displaces the RNA inhibitor effector by binding a single-stranded 6-nt overhang (toehold), thus restoring the affinity of the receptor for its ligand (Figure 2g).[44] We can modulate the loading of the DNA ligand to the receptor by varying the concentration of the "load" gene (0–300 nM) in the presence of a fixed concentration of "release" gene (1 nM) (Figure 2h, Figures Supporting Information 5, 6). Finally, the ligand's load and release from the receptor can be cycled multiple times by sequentially adding the "load" and "release" genes to a solution containing the receptor/ligand complex (Figure 2i).

Starting from the primary chemical reactions designed to occur among ligand, receptor, genetic components, and enzymes in the system, we built an Ordinary Differential Equation (ODE) model that generally captures the trends observed in experiments (reactions and ODEs are listed in Supporting Information section Supporting Information 3). The model was fitted to the kinetic data (Figures Supporting Information 2, 4, 6), obtaining parameters that align with the literature.[45] The simulation results are shown in gray in Figure 2c,e,h.

Next, we demonstrate the possibility to achieve cotranscriptional dynamic control of a ligand-binding DNA aptamer. As an illustrative example we used here the well-known ATP-binding aptamer.[46] More specifically, we employed a re-engineered version of the aptamer displaying an 18-nt loop domain connecting the ATP-binding portions.[23] The binding of a transcribed RNA strand to such loop domain induces the opening of the aptamer and the release of ATP (Figures Supporting Information 7, 8). To monitor the binding events in real-time, and thus ATP loading/release, the aptamer receptor was modified at both ends with a fluorophore and quencher pair (Figure 3a). When ATP is present in solution, it binds to the receptor

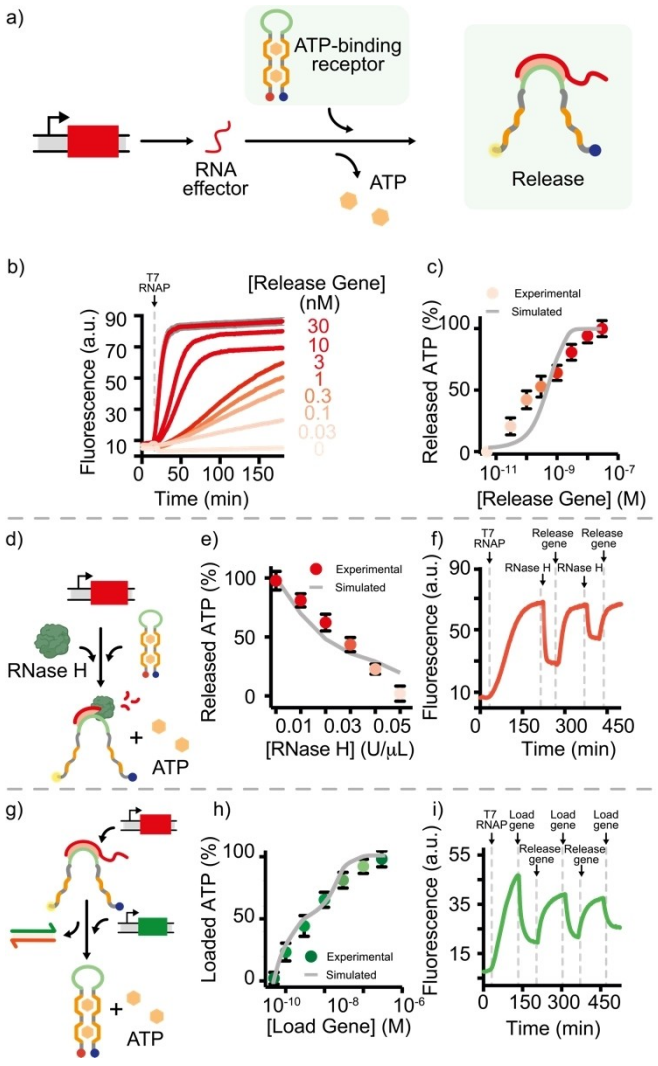

Figure 3. a) Schematic of our DNA aptamer-based receptor and its RNA effector. b) Time-course experiments showing the influence of varying the concentration of "release" gene. c) Plot showing the percentage of released ATP as a function of the "release" gene concentration (obtained from end points kinetic data like those shown in panel b). d) Scheme of the controlled release of the ATP in the presence of RNase H. e) Plot of the percentage of released ligand as a function of RNase H concentration (ranging from 0.05 U/μL to 0 U/μL) (time-course experiments are shown in Figure Supporting Information 11). f) Time-course experiments with sequential addition of RNase H (0.05 U/μL) and "release" gene (10 nM) after the first addition of T7 RNAP. g) Scheme representing the reversible load/release of ATP via strand displacement. h) Plot of the percentage of loaded ATP as a function of "load" gene concentration in the presence of a fixed concentration of "release" gene (1 nM) (time-course experiments are shown in Figure Supporting Information 14) i) Time-course experiments with sequential additions of "load" (30 nM) and "release" (10 nM) gene after the first addition of T7 RNAP. All transcription reactions were carried out using ATP aptamer receptor (50 nM), ATP (1 mM), T7 RNAP (4 U/μL). In the graphs, dots represent experimental values while solid gray lines represent fits (c, e, and h) obtained with the kinetic model (see Supporting Information Section Supporting Information 3.4, 3.5).

© 2024 Wiley-VCH GmbH

15213757, 2024, 17, Downloaded from https://onlinelibrary.wiley.com/doi/10.1002/ange.202319382 by University Of California, Los, Wiley Online Library on [29/09/2024]. See the Terms and Conditions (https://onlinelibrary.wiley.com/terms-and-conditions) on Wiley Online Library for rules of use; OA articles are governed by the applicable Creative Commons License

bringing the fluorophore and quencher into close proximity, thus resulting in a decrease of the fluorescence signal. In contrast, when the RNA inhibitor strand is transcribed by the corresponding "release" gene and binds to the receptor, it promotes the release of ATP and leads to an increase of fluorescence. We estimate the percentage (%) of ATP released through the relative fluorescence signal change registered upon RNA transcription.

Also in this case, the release of ATP from the aptamer receptor can be tuned by varying concentrations of RNase H (from 0 to 0.05 U/μL) (Figure 3d,e, Figures Supporting Information 9–12), using a fixed concentration of the "release" gene (30 nM). Sequential addition of the RNase H (0.05 U/μL) and "release" gene (10 nM) allows the reversible loading and release of ATP from the receptor (Figure 3f). To provide an additional means to control the loading and release of ATP from the ATP-binding receptor, we implemented the strand displacement strategy described earlier by engineering a "load" gene that produces an RNA strand acting as an activator (Figure 3g, Figure Supporting Information 13). By supplying different concentrations of the "load" gene (0–100 nM) it is possible to regulate cotranscriptionally the amount of receptor-bound ATP and restore the original binding ability of the aptamer (Figure 3h, Figures Supporting Information 14, 15). An advantage of the strand displacement strategy is that it can be repeated cyclically, by sequential addition of the same amount of "load" and "release" genes to a solution containing preformed receptor/ATP complex (Figure 3i). We finally fitted to the aptamer receptor data our general ODE model capturing the dynamics of receptor, ligand, and genetic regulators, again obtaining simulated dose-responses (shown in gray) that generally align with the data (SI section Supporting Information 3.5). A possible limitation of the above example regards the small change of ATP concentration after its release compared to the total ATP concentration in solution (1 mM). Despite this, the example remains in our opinion useful to demonstrate the validity of our approach, as the ATP-binding aptamer represents one of the best characterized binding-induced conformational-change aptamers.

We finally demonstrate a third class of DNA receptors (Figure 4a). In this case the receptor is designed to fold into a stem-loop hairpin structure that includes two tails flanking either end of the stem (orange portion, Figure 4).[26] The ligand-binding region of the receptor is however the loop domain (gray, Figure 4), which is designed to hybridize to a single-stranded DNA ligand (purple, Figure 4), and when the receptor is bound to its ligand, the formation of the stem is hindered. The addition of an inhibitor RNA strand targeting both receptor tails promotes the hybridization of the stem domains, and induces the release of ligand (Figure Supporting Information 16). Like in previous cases, to monitor the loading and release of the DNA ligand, we labeled the hairpin with a fluorophore/quencher pair. Binding of the DNA ligand to the hairpin results in a conformational change that pushes the fluorophore away from the quencher, resulting in an increase in fluorescence.

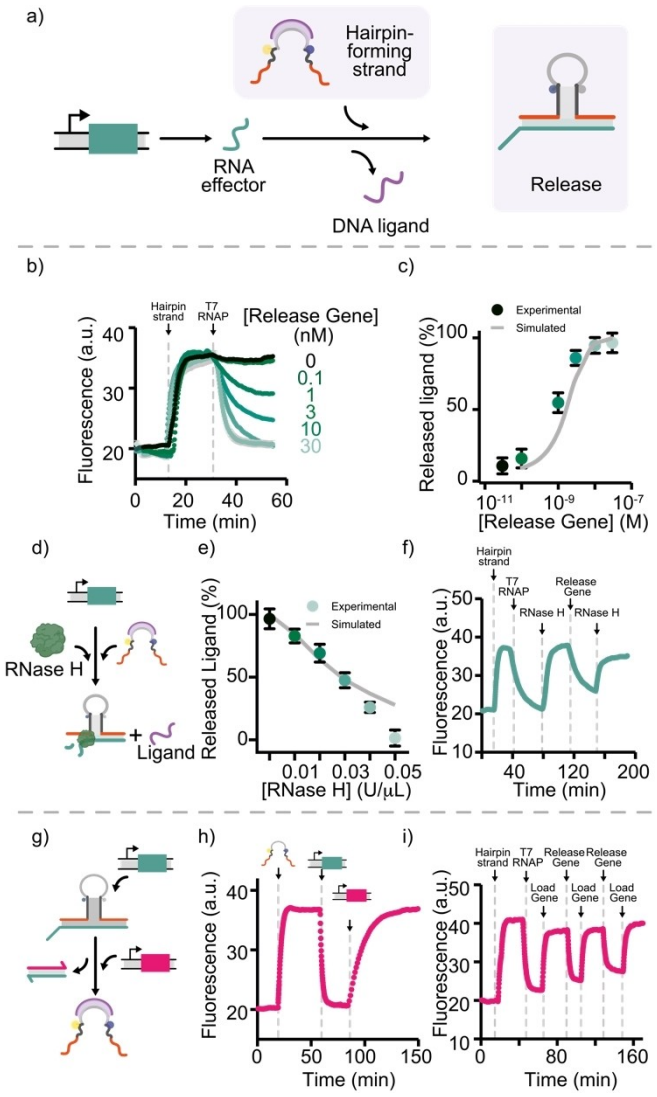

Figure 4. a) Scheme showing the operation of the DNA hairpin-based receptor system and its RNA effector. b) Time-course experiments testing different concentrations of the "release" gene. c) Plot of the percentage of released ligand as a function of the "release" gene concentration (endpoints of kinetics, example shown in b). d) Scheme of the controlled release of DNA ligand in the presence of RNase H. e) Plot of the percentage of released ligand as a function of RNase H concentration (ranging from 0 U/μL to 0.05 U/μL) (time-course experiments are shown in Figure Supporting Information 18) f) Time-course experiments with sequential addition of and RNase H (0.05 U/μL) and "release" gene (10 nM). g) Scheme of the reversible load/release of DNA target via strand displacement. h) The target loaded onto the receptor in the presence of a fixed concentration of "release" gene (10 nM) can be released by adding "load" gene at a concentration of 30 nM. i) Time-course experiments with sequential additions of "load" (10 nM) and "release" genes at concentrations of 30 and 10 nM. All transcription reactions were carried out using hairpin-forming strand (30 nM), DNA target (100 nM), T7 RNAP (4 U/μL). In the graphs, dots represent experimental values while solid gray lines represent fits (c, e) obtained with the kinetic model (see Supporting Information section Supporting Information 3.6, 3.7).

To cotranscriptionally control the receptor, we again developed a system of RNA effectors (inhibitors and

© 2024 Wiley-VCH GmbH

15213757, 2024, 17, Downloaded from https://onlinelibrary.wiley.com/doi/10.1002/ange.202319382 by University Of California, Los, Wiley Online Library on [29/09/2024]. See the Terms and Conditions (https://onlinelibrary.wiley.com/terms-and-conditions) on Wiley Online Library for rules of use; OA articles are governed by the applicable Creative Commons License

activators) that are transcribed by artificial genes. When the RNA inhibitor is produced, it stabilizes the stem-loop structure leading to the release of pre-loaded DNA ligand and to a decrease in the fluorescence signal. Like in previous cases, receptor inhibition occurs cotranscriptionally, thus we can control the release of the DNA ligand from the hairpin by varying the concentration of the "release" gene (Figure 4b,c, Figure Supporting Information 17). Also for this system, we observed a concentration-dependent decrease in ligand release through the combined use of RNase H and "release" gene (Figure 4d,e, Figure Supporting Information 18, 19). Our general ODE model initially failed to reproduce the kinetics of this receptor system; our fits significantly improved after including reactions that model the fact that distinct inhibitors could bind to the two branches of the receptor, leading to intermediate receptor states (SI section Supporting Information 3.6, 3.7).

Sequential additions of RNase H and "release" gene to a solution containing the receptor/ligand complex and T7 RNAP, allow for reversible and efficient load and release of the DNA ligand from the device (Figure 4f). Also in this case, a genetically encoded RNA activator complementary to the inhibitor can be used to regulate the receptor cotranscriptionally (Figure 4g). We demonstrated modulation of ligand reloading by using a saturating concentration of "load" gene (30 nM) and a fixed concentration of "release" gene (10 nM), (Figure 4h). Finally, cotranscriptional, sequential cycles of load and release of DNA ligand can be achieved by sequential addition of "release" and "load" genes (Figure 4i).

Conclusion

We reported a generalizable strategy to build dynamically controlled DNA receptors, whose capacity to load/release a target ligand is regulated cotranscriptionally by synthetic genes in vitro. Our demonstration includes three different DNA-based receptors that were rationally designed: a triplex-forming DNA-based receptor, an ATP-binding aptamer and a DNA hairpin receptor. We regulated their ability to bind a specific ligand cotranscriptionally, through RNA effectors produced by the synthetic genes in which they are encoded.

An important advantage of the dynamic nature of these receptors is that the effector sequence, which can be considered an input, is physically and chemically decoupled from the ligand, which can be considered an output. This is a sought-after property in ligand-binding supramolecular devices, as it allows for interconnecting the operation of molecules bearing completely distinct information encoded in their sequence. Further, the molecules released by the receptors may be used to regulate the production of the effectors, making it possible to build feedback loops. Our approach takes advantage of nucleic acid devices that are easy to design, build, and store, and of low-complexity cell-free conditions supporting transcription. Looking forward, our nucleic acid receptors may be conveniently adapted for load/release of a variety of other ligands (i.e., other RNA/DNA sequences, small molecules, and proteins), requiring simply a sequence redesign of the genetic elements producing the RNA effectors. More importantly, our receptors may be coupled to transcription-based devices in more complex samples. We envision that these receptors could respond to RNA transcribed in clinically relevant contexts, and contribute to the development of new methods for biosensing, point-of-care diagnostics and drug-release devices. Moreover, the high degree of controllability of the transcribed RNA offered by our approach may show potential for in vivo settings, such as the regulation of protein expression and activity, allowing precise control of cellular behavior.[47,48]

Supporting Information

The authors have cited additional references within the Supporting Information. Experimental methods, oligonucleotides sequences, kinetic model, curve fitting, and control and supporting experiments can be found in the Supporting Information (PDF).

Acknowledgements

This work was supported by the European Research Council, ERC (project n.819160) (FR), by Associazione Italiana per la Ricerca sul Cancro, AIRC (project n. 21965) (FR), by the Italian Ministry of University and Research (Project of National Interest, PRIN, 2022ANCEK). EF and EN acknowledge support from NSF award CCF 2107483.

Conflict of Interest

The authors declare no conflict of interest.

Data Availability Statement

The data that support the findings of this study are available from the corresponding author upon reasonable request.

Keywords: Synthetic receptors · DNA nanotechnology · enzymes · cell-free systems · synthetic biology

[1] A. D. Silverman, A. S. Karim, M. C. Jewett, *Nat. Rev. Genet.* **2019**, *21*, 151–170.
[2] S. M. Brooks, H. S. Alper, *Nat. Commun.* **2021**, *12*, 1–16.
[3] G. Mazzotti, D. Hartmann, M. J. Booth, *J. Am. Chem. Soc.* **2023**, *145*, 9481–9487.
[4] D. Hartmann, R. Chowdhry, J. M. Smith, M. J. Booth, *J. Am. Chem. Soc.* **2023**, *145*, 9471–9480.
[5] Y. Wu, Y. Li, K. Jin, L. Zhang, J. Li, Y. Liu, G. Du, X. Lv, J. Chen, R. Ledesma-Amaro, L. Liu, *Nat. Chem. Biol.* **2023**, *19*, 367–377.
[6] K. Pardee, *Biochem. Eng. J.* **2018**, *138*, 91–97.

© 2024 Wiley-VCH GmbH

15213757, 2024, 17, Downloaded from https://onlinelibrary.wiley.com/doi/10.1002/ange.202319382 by University Of California, Los, Wiley Online Library on [29/09/2024]. See the Terms and Conditions (https://onlinelibrary.wiley.com/terms-and-conditions) on Wiley Online Library for rules of use; OA articles are governed by the applicable Creative Commons License

[7] K. Pardee, S. Slomovic, P. Q. Nguyen, J. W. Lee, N. Donghia, D. Burrill, T. Ferrante, F. R. McSorley, Y. Furuta, A. Vernet, M. Lewandowski, C. N. Boddy, N. S. Joshi, J. J. Collins, *Cell* **2016**, *167*, 248–259.e12.
[8] M. P. McNerney, Y. Zhang, P. Steppe, A. D. Silverman, M. C. Jewett, M. P. Styczynski, *Sci. Adv.* **2019**, *5*.
[9] M. K. Takahashi, X. Tan, A. J. Dy, D. Braff, R. T. Akana, Y. Furuta, N. Donghia, A. Ananthakrishnan, J. J. Collins, *Nat. Commun.* **2018**, *9*, 1–12.
[10] M. Karlikow, S. J. R. da Silva, Y. Guo, S. Cicek, L. Krokovsky, P. Homme, Y. Xiong, T. Xu, M. A. Calderón-Peláez, S. Camacho-Ortega, D. Ma, J. J. F. de Magalhães, B. N. R. F. Souza, D. G. de Albuquerque Cabral, K. Jaenes, P. Sutyrina, T. Ferrante, A. D. Benitez, V. Nipaz, P. Ponce, D. G. Rackus, J. J. Collins, M. Paiva, J. E. Castellanos, V. Cevallos, A. A. Green, C. Ayres, L. Pena, K. Pardee, *Nat. Biomed. Eng.* **2022**, *6*, 246–256.
[11] C. H. Woo, S. Jang, G. Shin, G. Y. Jung, J. W. Lee, *Nat. Biom. Eng.* **2020**, *4*, 1168–1179.
[12] R. Lopez, R. Wang, G. Seelig, *Nat. Chem.* **2018**, *10*, 746–754.
[13] S. Slomovic, K. Pardee, J. J. Collins, *Proc. Natl. Acad. Sci. USA* **2015**, *112*, 14429–14435.
[14] A. A. Green, P. A. Silver, J. J. Collins, P. Yin, *Cell* **2014**, *159*, 925–939.
[15] K. Pardee, A. A. Green, T. Ferrante, D. E. Cameron, A. Daleykeyser, P. Yin, J. J. Collins, *Cell* **2014**, *159*, 940–954.
[16] J. K. Jung, K. K. Alam, M. S. Verosloff, D. A. Capdevila, M. Desmau, P. R. Clauer, J. W. Lee, P. Q. Nguyen, P. A. Pastén, S. J. Matiasek, J. F. Gaillard, D. P. Giedroc, J. J. Collins, J. B. Lucks, *Nat. Biotechnol.* **2020**, *38*, 1451–1459.
[17] A. Patino Diaz, S. Bracaglia, S. Ranallo, T. Patino, A. Porchetta, F. Ricci, *J. Am. Chem. Soc.* **2022**, *144*, 5820–5826.
[18] S. Bracaglia, S. Ranallo, F. Ricci, *Angew. Chem. Int. Ed. Engl.* **2023**, *62*, e202216512.
[19] S. Ranallo, S. Bracaglia, D. Sorrentino, F. Ricci, *ACS Sens.* **2023**, *8*, 2415.
[20] R. E. Rondon, T. M. Groseclose, A. E. Short, C. J. Wilson, *Nat. Commun.* **2019**, *10*, 1–13.
[21] B. D. Huang, T. M. Groseclose, C. J. Wilson, *Nat. Commun.* **2022**, *13*, 1–13.
[22] T. von der Haar, T. E. Mulroney, F. Hedayioglu, S. Kurusamy, M. Rust, K. S. Lilley, J. E. Thaventhiran, A. E. Willis, C. M. Smales, *Front. Mol. Biosci.* **2023**, *10*, 1128067.
[23] J. Kim, E. Winfree, *Mol. Syst. Biol.* **2011**, *7*, 465.
[24] A. Climent-Catala, T. E. Ouldridge, G.-B. V. Stan, W. Bae, *ACS Synth. Biol.* **2022**, *11*, 562–569.
[25] V. Mardanlou, C. H. Tran, E. Franco, **2014** 53rd IEEE Conference on Decision and Control, 4605–4610.
[26] H. Lee, T. Xie, X. Yu, S. W. Schaffter, R Schulman, **2023**, bioRxiv [preprint] doi: 10.1101/2023.08.10.552680.
[27] E. Del Grosso, A. Idili, A. Porchetta, F. Ricci, *Nanoscale* **2016**, *8*, 18057–18061.
[28] E. Del Grosso, I. Ponzo, G. Ragazzon, L. J. Prins, F. Ricci, *Angew. Chem. Int. Ed. Engl.* **2020**, *59*, 21058–21063.
[29] K. Eersels, P. Lieberzeit, P. Wagner, *ACS Sens.* **2016**, *1*, 1171–1187.
[30] L. Escobar, P. Ballester, *Chem. Rev.* **2021**, *121*, 2445–2514.
[31] R. A. Tromans, T. S. Carter, L. Chabanne, M. P. Crump, H. Li, J. V. Matlock, M. G. Orchard, A. P. Davis, *Nat. Chem.* **2018**, *11*, 52–56.
[32] J. Chen, R. J. Hooley, W. Zhong, *Bioconjugate Chem.* **2022**, *33*, 2245–2253.
[33] S. M. Douglas, I. Bachelet, G. M. Church, *Science* **2012**, *335*, 831–834.
[34] G. Grossi, M. Dalgaard Ebbesen Jepsen, J. Kjems, E. S. Andersen, *Nat. Commun.* **2017**, *8*, 1–8.
[35] M. Rossetti, E. Del Grosso, S. Ranallo, D. Mariottini, A. Idili, A. Bertucci, A. Porchetta, *Anal. Bioanal. Chem.* **2019**, *411*, 4293–4302.
[36] W. Engelen, C. Sigl, K. Kadletz, E. M. Willner, H. Dietz, *J. Am. Chem. Soc.* **2021**, *143*, 21630–21636.
[37] H. Ijäs, I. Hakaste, B. Shen, M. A. Kostiainen, V. Linko, *ACS Nano* **2019**, *13*, 5959–5967.
[38] F. Ricci, A. Vallée-Bélisle, A. Porchetta, K. W. Plaxco, *J. Am. Chem. Soc.* **2012**, *134*, 15177–15180.
[39] J. L. Vinkenborg, N. Karnowski, M. Famulok, *Nat. Chem. Biol.* **2011**, *7*, 519–527.
[40] E. A. Phillips, A. D. Silverman, A. Joneja, M. Liu, C. Brown, P. Carlson, C. Coticchia, K. Shytle, A. Larsen, N. Goyal, V. Cai, J. Huang, J. E. Hickey, E. Ryan, J. Acheampong, P. Ramesh, J. J. Collins, W. J. Blake, *Nat. Biom. Eng.* **2023**, 1–12.
[41] D. Mariottini, A. Idili, A. Vallée-Bélisle, K. W. Plaxco, F. Ricci, *Nano Lett.* **2017**, *17*, 3225–3230.
[42] A. F. Rodríguez-Serrano, I. M. Hsing, *ACS Synth. Biol.* **2021**, *10*, 371–378.
[43] A. Porchetta, A. Idili, A. Vallée-Bélisle, F. Ricci, *Nano Lett.* **2015**, *15*, 4467–4471.
[44] J. Lloyd, C. H. Tran, K. Wadhwani, C. Cuba Samaniego, H. K. K. Subramanian, E. Franco, *ACS Synth. Biol.* **2018**, *7*, 30–37.
[45] M. Weitz, J. Kim, K. Kapsner, E. Winfree, E. Franco, F. C. Simmel, *Nat. Chem.* **2014**, *6*, 295–302.
[46] D. E. Huizenga, J. W. Szostak, *Biochem.* **1995**, *34*, 656–665.
[47] F. Sedlmayer, D. Aubel, M. Fussenegger, *Nat. Biomed. Eng.* **2018**, *2*, 399–415.
[48] A. P. Teixeira, M. Fussenegger, *Adv. Sci.* **2013**, *11*, 2309088.

Manuscript received: December 15, 2023
Accepted manuscript online: March 8, 2024
Version of record online: March 22, 2024

© 2024 Wiley-VCH GmbH

15213757, 2024, 17, Downloaded from https://onlinelibrary.wiley.com/doi/10.1002/ange.202319382 by University Of California, Los, Wiley Online Library on [29/09/2024]. See the Terms and Conditions (https://onlinelibrary.wiley.com/terms-and-conditions) on Wiley Online Library for rules of use; OA articles are governed by the applicable Creative Commons License